Thrust Vectoring of Multiaperture Cesium Electron Bombardment Ion Engines

V. V. Fosnight,* T. R. Dillon,† and G. Sohl‡
Electro-Optical Systems, A Division of Xerox Corporation, Pasadena, Calif.

Thrust vectoring of a 100 μlb multiaperture cesium electron bombardment engine through an angle of ±5° by the method of accelerator displacement has been previously reported. The limit of thrust deflection on that engine was determined by the rise in accelerator current as ions struck the displaced accelerator. The effects on the thrust deflection limit of accelerator aperture diameter and shape, accel thickness, electrode spacing, screen electrode geometry, and ion beam focusing voltages are described. Optimization of these results has provided a thrust deflection capability of ±9° in two orthogonal axes with the same 100 μlb engine used before. The stability and lifetime effects of large angle deflections are described, and time response data are presented.

Introduction

THE accelerator displacement method of thrust vectoring multiaperture electron bombardment ion engines through angles of ±5° was described in Ref. 1. In this method thermal expansion forces were used to translate the accelerator of a cesium bombardment microthruster perpendicular to the thruster axis and to thus deflect the exhaust ion beams. Reference 2 describes the applications (north-south station keeping and active attitude control) of a microthruster system with this thrust vectoring capability. This paper describes the results of experiments to increase the angular limit of thrust vectoring.

The experiments reported here include evaluations of modifications to the electrode geometry and the deflection on ion beam focusing and the plasma boundary. Stability of the thruster and of the deflected thruster vector was studied, and time response measurements were made.

The 100 μlb cesium electron bombardment microthruster[2] with 19 aperture electrodes shown in Fig. 1 was used for all testing. The accelerator is mounted from four radial insulators from the front ring at ground potential, so all of the thrust deflection system components are held near ground potential to eliminate extra high-voltage components. The front ring also electrically connects the eight thermal expansion elements mounted in pairs between the front and rear rings.

Accelerator Electrode Geometry Tests

The limit of practical thrust deflection as a function of the accelerator aperture diameters and shapes, and of the accelerator thickness, was measured using an *XYZ* collector.[1] Calibration of the *XYZ* collector is shown in Fig. 2. In order to compare all of the data directly, the thrust deflection limit was defined as the angle between the engine axis and the deflected thrust vector when the accelerator drain current increased to 0.50 ma, or approximately five times its zero deflection value. For nearly all of the data the beam current at zero deflection was 6.0 ma and the thrust was 100 μlb.

Received April 14, 1969; revision received November 3, 1969. Work supported by Air Force Aero Propulsion Laboratory, Wright-Patterson Air Force Base, under Contract F33615-67-C-1268.

* Physicist, Aerospace Systems Division.
† Associate Engineer, Aerospace Systems Division.
‡ Senior Engineer. Member AIAA.

The data were taken by plotting the accelerator drain current as a function of the *XYZ* collector output on an *xy* plotter as the thrust vector was varied by displacing the accelerator mounted on the thrust deflection system. The collector output is proportional to the sine of the deflection angle. The traces taken in this manner are u-shaped curves with the drain current showing a broad minimum over most of the deflection range and rising sharply at each side of the minimum. These rapid drain current increases are caused by direct interception of beam ions by the sides of the accelerator apertures and are the limiting factors in the possible angle of the thrust deflection.

Accelerator Aperture Size

Figure 3 shows the *xy* recorder traces for accelerator aperture diameters of 0.086 and 0.095 in. The calculated thrust deflection angles at 0.50 ma drain current are ±3.65 and ±5.43 degrees of arc, respectively. Thus, the thrust deflection limit can be increased by merely increasing the ac-

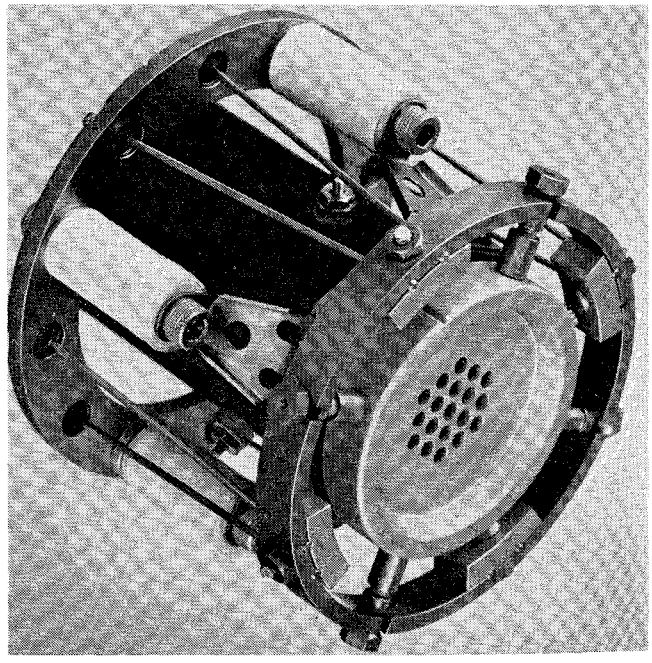

Fig. 1 100μ lb thruster with thrust deflection system.

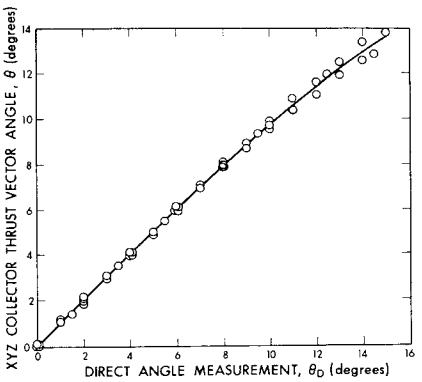

Fig. 2 *XYZ* collector calibration.

celerator aperture diameter to delay interception of the deflected ion beam. A disadvantage of the larger apertures is a slight loss of electrode perveance due to the aperture effect. Both traces in Figure 3 were taken with a positive high voltage of 2.00 kv and a negative high voltage of 0.8 kv. These negative high voltages were 0.2 kv higher than required for the smaller 0.086-in.-diam apertures.

Accelerator Aperture Shape

To limit the aperture effect and still raise the thrust deflection limit by delaying the ion interception by the accelerator, the accelerator apertures were countersunk from the downstream side of the electrode to within 0.020 in. of the gap side. The aperture diameters at the gap side of the accelerator for the three countersunk electrodes tested were 0.086 in. Figure 4 gives the deflection traces taken with total countersink angles of 0, 15, 30, and 45°. The positive and negative high voltages used in each test were 2.00 and 0.60 kv, respectively. The beam currents were 6.0 ma (100 μlb), and the interelectrode gap was 0.063 in. Table 1 shows the thrust vector angle at 0.50 ma drain current. Also shown is the angle at 0.20 ma drain current which could be used as a limit to insure extremely stable operation. The 4° countersunk electrode showed the highest deflection limit of ±7.36°. A larger countersink would probably increase this limit even more, but the web between apertures for the 45° and larger countersinks would be small and would tend to limit accelerator life. The chief advantage of the countersunk electrodes over an electrode with enlarged apertures is that there is no loss of perveance since the accelerator geometry on the side nearest the screen electrode is not changed.

The effects of accelerator thickness on the 30° countersunk electrode was examined by measuring the thrust deflection angle limit on a 0.061 in.-thick and a 0.100-in.-thick accelerator. At the drain current limit of 0.50 ma the calculated thrust vector angles were 6.40 and 6.58°, respectively, for the

Table 1 Thrust deflection angle for countersunk accelerators

Aperture Diameter, in.	0.086	0.086	0.086	0.086
Countersink Angle, deg	0	15	30	45
Positive High Voltage, kv	2.00	2.00	2.00	2.00
Negative High Voltage, kv	0.60	0.60	0.60	0.60
Beam Current, ma	6.0	6.0	6.0	6.0
Thrust Vector Angle at 0.50 ma Drain Current Limit, deg	±3.00	±5.96	±6.58	±7.71
Thrust Vector Angle at 0.20 ma Drain Current, deg	±2.89	±5.61	±6.13	±7.36

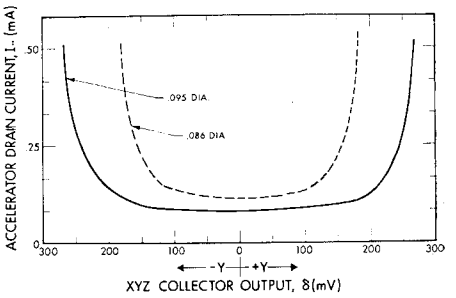

Fig. 3 Thrust deflection for different aperture diameters.

0.100 in. accelerators. The 2.8% deflection increase with the thicker electrode is almost negligible when compared to the accuracy of the measurements (±2.5%). No significant increase with the thicker electrode should be expected because of the very high ion momentums while passing through the accelerator apertures.

Ion Beam Focusing

In all of the accelerator geometry tests, the focusing of the individual ion beams passing through each aperture pair was studied. As noted earlier the effect of enlarging or countersinking the accelerator apertures was to delay the ion interception by the sides of the accelerator apertures until a larger exhaust beam angle was reached. Because of the success of the countersinking, it must be assumed that the ion beams focused through the accelerator apertures first started to impinge on the accelerator on the walls of the apertures at the exhaust side of the electrode as the thrust vector limit was reached. But the countersinks did not focus the beams more sharply. Sharper focused or more narrow beams are desirable to further delay the interception. Because the extraction of ions from an electron bombardment thruster is governed by space charge limited current conditions, the focusing depends on the electrode spacing, screen aperture shape, screen thickness, the positive and negative high voltages and the plasma density within the ion source. These factors establish a plasma boundary at the screen electrode apertures whose shape and position varies with each of the aforementioned parameters.

Given a desired thrust the plasma density is nearly invariant (depending somewhat on the electrode geometry) and cannot be changed just to improve the focusing to increase the thrust vectoring limit. The other parameters can be varied to decrease the cross section area of the ion beams as they pass through the accelerator. These parameters are considered in turn.

Electrode Gap

The effects of electrode gap on the limit of thrust deflection were investigated using both the 30° and the 45° countersunk accelerators. The drain current was plotted as a func-

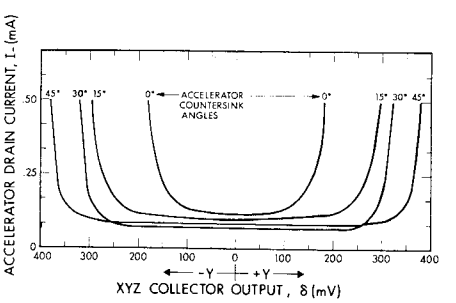

Fig. 4 Thrust deflection for different aperture countersink angles.

Table 2 Thrust deflection angles for different electrode gaps

Electrode Gap, in.	0.063	0.059	0.055	0.070	0.063	0.059	0.055	0.50
Countersink Angle, deg	45	45	45	30	30	30	30	30
Aperture Diam, in.	0.086	0.086	0.086	0.086	0.086	0.086	0.086	0.086
Positive High Voltage, kv	2.00	2.00	2.00	2.00	2.00	2.00	2.00	2.00
Negative High Voltage, kv	0.60	0.60	0.60	0.60	0.60	0.60	0.60	0.60
Beam Current, ma	6.0	6.0	6.0	6.0	6.0	6.0	6.0	6.0
Thrust μlb	100	100	100	100	100	100	100	100
Vectoring Angle at 0.50 ma Limit, deg	±7.71	±8.00	±9.90	±5.27	±6.58	±8.36	±9.17	±10.87
Vectoring Angle at 0.20 ma, deg	±7.34	±7.28	±9.64	±4.24	±6.53	±7.77	±8.28	±10.45

tion of the XYZ collector output for interelectrode spacings of 0.063, 0.059, and 0.055 in. for the 45° countersunk accelerator, and spacings of 0.070, 0.063, 0.059, 0.055, and 0.050 in. for the 30° countersunk electrode. Table 2 summarizes the results of the tests both for the 0.50 and 0.20 ma drain current intercepts. The smaller gaps gave a much higher thrust deflection limit for the same positive and negative high voltages and beam current because the individual ion beams were better focused by the higher electric fields. Therefore, the ion beams were much narrower as they passed through the accelerator apertures, so more accelerator displacement was required before the rise in direct ion interception was reached.

The higher electric fields with the gap less than 0.050 in. caused an over-focused condition with the focus spot too close to the screen electrode, so that the sharp increase of the drain current at the vectoring limit gave way to a gradual increase throughout the entire vectoring range. This poor drain current characteristic would lead to more accelerator wear for very long operating periods. Therefore, for the test microthruster requiring 2.0 kv positive high voltage for 100 micropounds thrust, a negative high voltage of 0.6 kv and a gap of between 0.50 and 0.055 in. gave the best results.

Screen Electrode Geometry

The screen electrode geometry was varied to measure its effect on the thrust deflection limit. The 0.100-in.-diam apertures in the screen electrode were not changed, thus keeping the electrode perveance required for 100 μlb thrust. The screen electrode apertures on the cesium bombardment thruster are normally countersunk 90° toward the plasma within the discharge chamber to approximate a thin screen electrode and obtain high perveance and stable operation.[3] Since the thin screen approximation tends to decrease the effective electrode spacing, screen electrode countersink angles of 0°, 60°, 90°, and 120° were tested. The gap was 0.057 in. except that a 0.055-in. gap was used for the 90° countersink data (reproduced from earlier tests). The total increase in thrust deflection limit from no countersink to a countersink angle of 90° was less than 1°. The 120° countersink was not significantly better than the 90° countersink. Therefore, a countersink angle of at least 90° is desirable for maximum deflection, but a larger angle is not necessary.

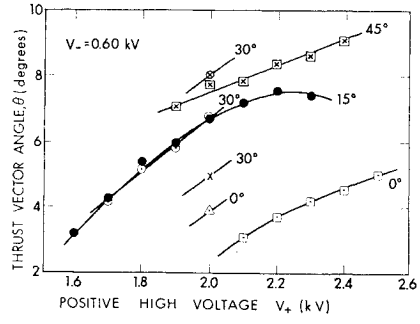

Fig. 5 Thrust deflection angle vs positive high voltage.

A 0.010-in.-thick screen electrode was tested for comparison to the former thickness of 0.025 in. The apertures were not countersunk. With an electrode gap of 0.057 in. the thrust vector angle at the 0.50 ma drain current limit was ±10°. This is an increase of nearly 1° over the best countersunk screens tested with the same gap. However, some sacrifice in the drain current characteristic with increasing angle was seen because of overfocusing as described above. With a larger electrode gap the thin screen is not superior to the 90° countersunk screen. The countersunk screens have an added advantage in applying the accelerator deflection method of thrust vectoring to larger engines because the extra thickness of the electrode web supplies needed mechanical strength for those engines where it was not needed for the 1-in.-diam thruster used in these tests.

Positive and Negative High Voltage

In the tests of the four different accelerator countersinks described previously the thrust deflection limit was measured as the high voltages were varied. Figures 5 and 6 show the thrust vector angle at a drain current of 0.50 ma plotted vs one high voltage with the other constant. The key for the data point symbols is given in Table 3. In general, Figs. 5 and 6 illustrate that the thrust vector angle is increased linearly for an increase in either high voltage, because up to a certain point the higher voltage causes a more concave plasma meniscus at the screen electrode which gives better focused ion beams through the accelerator electrode. The same effect can be seen for the low and high beam current points plotted. For the 5.0 and 7.0 ma beam currents the thrust deflection angle is respectively higher and lower than with a 6.0 ma beam for the same voltages. With a given screen electrode geometry and electrode gap the plasma density within the discharge chamber is varied to change the beam current that is extracted from the plasma boundaries since the thruster always operates in the space charge limited mode. A lower plasma density (lower beam current), therefore, leads to a more concave meniscus and better beam focusing in just the same way as an increase in either high voltage gives better focusing.

For the gap tests described earlier the thrust deflection limit at the 0.50 ma drain current limit is plotted vs the negative high voltage for the five gaps in Fig. 7. The positive high voltage was 2.00 kv and the beam current was 6.0 ma

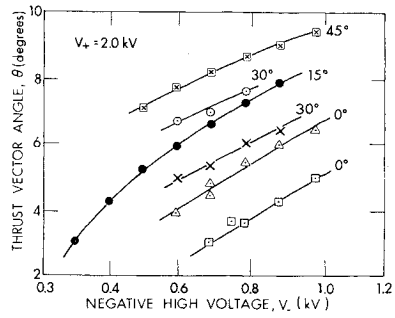

Fig. 6 Thrust deflection angle vs negative high voltage.

Table 3 Key for data points in Figs. 5 and 6

Symbol	Aperture diam.	Countersink angle	Electrode spacing	Beam current
⊡	0.086 in.	0°	0.063 in.	6.0 ma
△	0.095 in.	0°	0.063 in.	6.0 ma
×	0.086 in.	30°	0.063 in.	7.0 ma
●	0.086 in.	15°	0.063 in.	6.0 ma
⊙	0.086 in.	30°	0.063 in.	6.0 ma
⊠	0.086 in.	45°	0.063 in.	6.0 ma
⊗	0.086 in.	30°	0.063 in.	5.0 ma

for all the curves ($T = 100$ μlb). These data illustrate the same focusing effects due to plasma meniscus shape and position changes as were found for the different accelerator geometries.

Comparison of Figs. 5, 6, and 7 also show that the ratio of the positive to negative high voltage over a wide range has only a slight effect on the thrust vector angle limit. This is because under the space charge limited current conditions present in the accelerating region, the plasma boundary position is established only by the electrode geometry, the plasma density, and the total applied voltages between the electrodes.

To determine if the thrust deflection angular sensitivity to the accelerator displacement varied with either high voltage, the accelerator was displaced to a set position, and the high voltages were separately varied as the XYZ collector output was measured. Figure 8 shows that as the negative high voltage was raised the thrust vector angle increased until a region of constant deflection was reached. This increase in angle for a constant accelerator position is apparently due to changes in the shape of the plasma boundary other than the gross curvature changes described before. The variation is only noted at reduced voltages where the ion sheath is closer to the accelerator and can be distorted asymmetrically. This distortion appears to counter the effects of accelerator displacement.

The same effect is seen on the left sides of the curves in Fig. 9 where the electrode displacement and negative high voltage were held constant as the positive high voltage was increased. On the curves of Fig. 9, however, the maximum deflection region is much narrower than for the varying negative high voltage. This is probably due to several effects. The aperture effect is important since it causes the accelerator potential to have a smaller effect than the same change in the positive high voltage. The decrease in sensitivity for the higher positive potentials is also caused by the increase in the effective gap. This together with the overfocusing just described is the reason for the leveling out of the thrust vector limit angles for those high voltages in Figs. 5 and 9. The same effects can be seen in Fig. 7 on the curves taken with small gaps. These results argue against increasing the thrust vector limit by simply raising either high voltage. An even more compelling argument against excessive positive high voltage is that the thrust is proportional to the beam

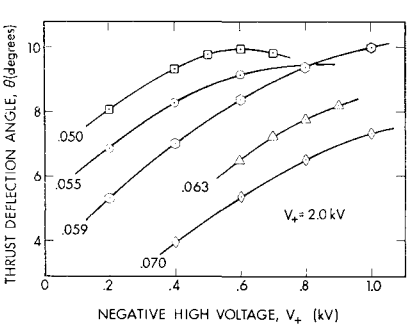

Fig. 7 Thrust deflection angle for different electrode spacings.

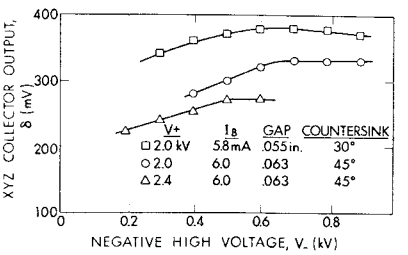

Fig. 8 Thrust deflection vs negative high voltage

current, I_B, times the square root of v_+ while the beam power is equal to $v_+ I_B$. Therefore, such a procedure is very costly in terms of system power required for a given thrust. The loss of vectoring sensitivity is not as severe with the negative potential, but a high v_- is costly in terms of lifetime due to both direct and charge exchange ion impingement on the accelerator.[4]

Thruster Stability

No loss of thruster stability was observed throughout the thrust vectoring tests. Stable discharge and extraction characteristics were typical over the entire range of thrust vectoring. No high-voltage sparking was found as a result of the vectoring process. Attainment of any desired thrust vector angle within the 0.50 ma drain current limit was easily and smoothly accomplished with no significant fluctuations in the vector angle or in any other thruster parameters. All of the testing was performed with the prototype thrust deflection system which keeps all of the thrust vectoring components at ground potential. No problems with this design were found. Furthermore, a flight-type package shroud was never used to surround the engine, and under these conditions the system seemed to have no dependence on external heat sources or thermal surfaces.

To detect any changes in the thrust vector angle due to accelerator wear, the thrust vector angle was set at 8° with a constant set of engine parameters, and the XYZ collector output was monitored periodically over a 24 hr period. The change in XYZ collector output with time was small and largely random indicating that the angle was constant at least to the accuracy of the measurements. Slight changes in the beam current were probably as instrumental in the output signal changes as any angular change. Comparison of accurate measures of the thrust vector angle limit before and after the test showed a net increase in the limit of about 0.3° which is near the limits of the experimental error. Examination of the accelerator after the test showed no significant amount of erosion in the direction of the deflected beam. Thus, it appears that any change in the thrust vector angle could only be determined by extended periods of vectoring at large angles. More sensitive tests of longer duration would have to be performed to determine more accurately the quantitative effects of such operation.

Time Response

Thrust vectoring response time measurements with the prototype thrust deflection system were made. Figure 10 shows the thrust vector limit in the $+x$ direction as measured by the XYZ collector plotted vs the rise or decay time for

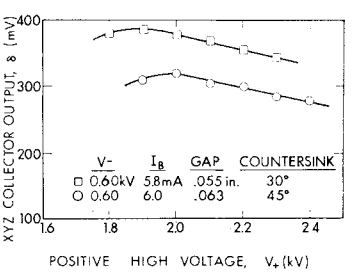

Fig. 9 Thrust deflection vs positive high voltage.

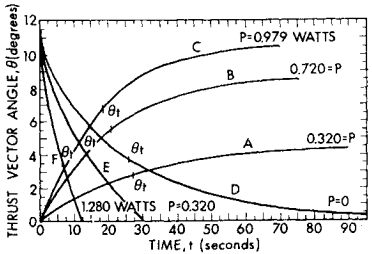

Fig. 10 Thrust deflection response.

several different power inputs. Data to draw the curves were taken every 5 sec except for curves E and F where the data were recorded at 2-sec intervals. Curves A, B, and C are exponential rise curves where at $t < 0$ the deflection power was zero. At $t = 0$ the power as noted was applied and held throughout the length of the curve. Curve D is an exponential decay curve where at $t = 0$ the power was removed. In curves E and F, at $t = 0$ the deflection power was turned off and the powers shown were applied to the opposite legs to speed the accelerator return. Therefore, E and F are probably combinations of two exponential functions, an exponential rise (of the power applied to the opposite legs) and an exponential decay of the cooling legs. The θ_t on the curves are the angles at which the $1/e$ values of θ occur, so for the pure exponential curves they indicate the time constant, t, in seconds. For the simple exponential curves time constants between 18 and 26 sec were found for the rising curves, and the time constant for the simple cooling decay was 26 sec. These time constants are very short compared to typical thrusting times for some satellite mission requirements.[2]

Conclusions

The range of thrust vectoring using displacement of the accelerator to deflect the ion beams expelled from a multiaperture electron bombardment thruster has been increased to $\pm 9°$ in two orthogonal axes. The thruster stability under all thrust deflection conditions was excellent. The time constant of the thrust vector angle with a flight prototype thrust deflection system was about 20 sec, and this time is very short compared to thrusting periods of some flight applications such as N-S station keeping.[2]

References

[1] Sohl, G. and Fosnight, V. V., "Thrust Vectoring of Ion Engines," *Journal of Spacecraft and Rockets*, Vol. 6, No. 2, Feb. 1969, pp. 143–147.

[2] Fosnight, V. V. et. al., "A Cesium Electron-Bombardment Microthruster System," AIAA Paper 69-293, Williamsburg, Va., 1969.

[3] Sohl, G., Speiser, R. C., and Wolters, J. A., "Life Testing of Electron-Bombardment Cesium Ion Engines," AIAA Paper 66-233, San Diego, Calif., 1966.

[4] Fosnight, V. V. et. al., "Cesium Ion Engine System Life Test Results," *Journal of Spacecraft and Rockets*, Vol. 5, No. 4, April 1968, pp. 465–467.